A Physical Basis of the Slip-wall Model for Wall-modeled Large-eddy Simulations

Xiang I. A. Yang

Center for Turbulence Research,
Stanford University,
488 Escondido Mall, Stanford, CA 94305, USA
xiangyang@stanford.edu

Sanjeeb T. Bose

Center for Turbulence Research,
Stanford University,
488 Escondido Mall, Stanford, CA 94305, USA
stbose@stanford.edu

ABSTRACT

Conducting large-eddy simulations (LES) implies the use of LES filters, which are commensurate with the local grid spacing. For wall modeled LES (WMLES) where the grid spacing in the wall-normal direction scales with the local boundary layer height, the near-wall turbulence is typically not well resolved. Because of the poorly-resolved near-wall region, the no-slip condition no longer applies; and a near-wall closure (an LES wall model) must be used. Recently S. T. Bose & P. Moin (Physics of Fluids, 26, 015104, 2014, *DOI: http://dx.doi.org/10.1063/1.4849535*) proposed to use a Robin-type near-wall closure $u_i - l_p \partial u_i/\partial y = 0$, where u_i's are the slip velocities at the wall, l_p is a slip length and the subscript $i = 1$, 2, 3 indicate the streamwise, wall-normal and spanwise directions respectively. Different from most physics-based LES wall models, this slip wall model is based on the use of a differential LES filter. In the present work, we provide a physics-based interpretation for this Robin-type wall closure. We show that the model is compatible with arbitrary LES filter and it can be motivated by the same considerations that lead to the equilibrium wall model. The possibility of explicitly accounting for non-equilibrium effects is briefly discussed. The model is tested in turbulent channel flow and its performance is compared against other wall models. The flow quantities of interest here include the mean velocity, the variance of the streamwise velocity fluctuation and the instantaneous wall shear stress.

INTRODUCTION

The need for LES wall models comes from the strict near-wall-resolution requirements of a wall-resolved LES (Chapman, 1979; Choi & Moin, 2012), the limited computational power and the need for high-fidelity numerical solutions in real-world engineering practices. Conducting large-eddy simulations (LES) implies the use of LES filters. The sizes of the LES filters are commensurate with the local LES grid spacing. For wall-modeled LES (WMLES), where the grid spacing in the wall-normal direction scales with the boundary layer height, the near-wall turbulence is poorly resolved. Because of this, the no-slip condition does not apply at the wall; and the wall boundary condition must be supplied by an LES wall model.

In general, there are at least three types of LES wall models (1) Dirichlet-type wall model, (2) Neumann-type near-wall closure and (3) Robin-type slip wall model (see Piomelli & Balaras (2002) for a review of commonly used LES wall models). A Dirichlet-type wall model provides a slip velocity u_w at the (virtual) wall (Bazilevs & Hughes, 2007; Chung & Pullin, 2009). Given a slip velocity and a non-vanishing eddy viscosity at the (virtual) wall, the wall shear stress can be computed in the same manner as it is in the bulk region. Neumann-type models provide the wall shear stress directly but the velocity at the wall is not explicitly modeled. This type of near-wall closure is probably the most intuitive and the most commonly used. It includes the algebraic wall models that are based on the law of wall (Schumann, 1975; Porté-Agel *et al.*, 2000), the algebraic integral wall model that solves the vertically integrated momentum equation (Yang *et al.*, 2015), the zonal wall models that integrate the Reynolds Averaged Navier Stokes (RANS) momentum and energy equation on a refined one-dimensional mesh between the wall and a wall-model/LES matching location (Balaras & Benocci, 1994; Park & Moin, 2014) and a number of models that rely on optimal control strategies and data mining techniques (Nicoud *et al.*, 2001; Templeton *et al.*, 2006). The use of Robin-type near-wall closures is not until quite recent and the first attempt is by Bose & Moin (2014), where they proposed to use the following wall condition in WMLES

$$\left[u_i - l_p \frac{\partial u_i}{\partial y}\right]_{y=0} = 0, \tag{1}$$

where $y = 0$ is at the wall. In Bose & Moin (2014) the slip length l_p is computed dynamically according to a Germano-like identity. As has been rigorously proved in Bose & Moin (2014), the slip wall formalism conforms with the use of the differential filter in LES (see Bose & Moin (2014) for detailed discussion). It is not clear, however, how the slip wall model captures the flow physics.

In this work, we provide a physics-based interpretation for this slip wall closure. We show first that the Robin-type wall closure is compatible with arbitrary LES filter, and second that the slip wall model can also be motivated using RANS-type equilibrium arguments. We would discuss briefly the possibility of explicitly accounting for the effects of flow acceleration and local pressure gradient in the slip wall model. The performance of the slip wall model is then compared against that of the integral wall model (see Yang *et al.* (2015) for details of the model) and the algebraic equilibrium wall model,

$$\tau_{w,x} = \left[\frac{\kappa u_{||}}{\log(h_{wm}/y_o)}\right]^2 \frac{u_{LES}}{u_{||}},\ \tau_{w,z} = \left[\frac{\kappa w_{||}}{\log(h_{wm}/y_o)}\right]^2 \frac{w_{LES}}{u_{||}}, \tag{2}$$

in turbulent channel flow, where $\kappa = 0.4$ is the Karman constant, τ_w is the wall shear stress, u_{LES}, v_{LES} are the LES velocity at $y = h_{wm}$, $u_{||} = \sqrt{u_{LES}^2 + w_{LES}^2}$ is the wall-parallel velocity, h_{wm} is the wall-model/LES matching height and y_o is the viscous/roughness length scale. The wall model solution matches with the spatially filtered LES solution at $y = h_{wm}$ (Bou-Zeid *et al.*, 2004). Throughout the article, we use x, y, z for the streamwise, wall-normal, and spanwise directions and u, v, w for the streamwise, wall-normal and spanwise velocities. The flow quantities of interest include the mean velocity and the variance of the streamwise velocity fluctuation. In addition, the probability density functions (p.d.f.) of the wall shear stress in WMLES and in filtered direct numerical simulations (DNS) are compared.

A PHYSICS-BASED INTERPRETATION FOR THE SLIP MODEL

In this section, we provide a physics-based interpretation for the slip wall closure. We begin with the law of wall

$$\frac{\langle u \rangle}{u_\tau} = \frac{1}{\kappa} \ln\left(\frac{y}{y_o}\right), \tag{3}$$

where u_τ is the friction velocity and $\langle \cdot \rangle$ indicates ensemble average. Imposing this log scaling instantaneously and locally, and matching it with the LES velocity at the first (or the second, third, etc. depending on the implementation (Kawai & Larsson, 2012)) grid point away from the wall leads to

$$u_\tau = \frac{\kappa u_{\text{LES}}}{\ln(h_{wm}/y_o)}. \tag{4}$$

Imposing again the law of wall and modeling the Reynolds stress using an eddy viscosity

$$\widetilde{u}\widetilde{v} - \tilde{u}\tilde{v} = \nu_T \frac{\partial u_{\text{LES}}}{\partial y} = u_\tau^2, \tag{5}$$

where ν_T is the eddy viscosity and the viscous stress is neglected. Substituting Eq. (4) into Eq. (5),

$$u_{\text{LES}} - \left[\frac{\ln(h_{wm}/y_o)\nu_T}{\kappa u_\tau}\right] \frac{\partial u_{\text{LES}}}{\partial y} = 0. \tag{6}$$

Equation (6) conforms with a Robin boundary condition and the slip length is

$$l_p = \frac{\ln(h_{wm}/y_o)\nu_T}{\kappa u_\tau}. \tag{7}$$

For a typical WMLES, where the $y = h_{wm}$ is in the log region, the eddy viscosity can be modeled via the mixing length model

$$\nu_T = \kappa h_{wm} u_\tau, \tag{8}$$

and according to Eq. (7)

$$l_p = h_{wm} \ln\left(\frac{h_{wm}}{y_o}\right). \tag{9}$$

Equations (6), (7) justify the use of a Robin-type condition in WMLES.

THE SLIP WALL MODEL

The physics-based interpretation in the previous section can be tested in WMLES. To do that we impose

$$u - l_p \frac{\partial u}{\partial y} = 0, \quad w - l_p \frac{\partial w}{\partial y} = 0, \quad v = 0 \tag{10}$$

at the wall with l_p specified according to Eq. (9). This Robin-type near-wall closure does not admit penetration at the wall. As a result, the momentum loss at the wall is entirely due to $\nu_T \partial u/\partial y$. This treatment is different from Bose & Moin (2014), in which a penetration condition is used and part of the momentum loss at the wall is due to a non-zero Reynolds stress $\langle u'v' \rangle$. As this work is to provide a physical basis for the Robin-type boundary condition in general, we do not necessarily need to conform with the exact formulation of Bose & Moin (2014).

The discussion so far has been based on equilibrium considerations. Non-equilibrium effects including flow acceleration and local pressure gradient can be explicitly accounted for by including a non-equilibrium correction to the otherwise equilibrium wall shear stress according to

$$\tau_{w,x}^{NE} = \tau_{w,x}^{E} + \tau_{w,x}^{c}, \tag{11}$$

where the superscript "E" indicates "equilibrium", "NE" indicates "non-equilibrium", "c" indicates "correction" and the subscript x indicates quantities in the flow direction. The wall stress in the spanwise direction can be corrected in the same manner. Following Yang *et al.* (2015), $\tau_{w,x}^{c}$ is

$$\tau_{w,x}^{c} = r\left[\int_{y=0}^{h_{wm}} -\frac{\partial p}{\partial x} - \frac{du}{dt} dy\right], \tag{12}$$

where $d\cdot/dt$ is the material derivative, p is the dynamic pressure, the pre-factor r is to resolve the time scale mismatch between the resolved eddies (of scale h_{wm}) and the filtered wall shear stress. Following Yang *et al.* (2015),

$$r = \frac{T_c}{T_w}, \tag{13}$$

where $T_c = \Delta_y/u_{\text{LES}}$ is the convective time scale, $T_w = \Delta_y/(\kappa u_\tau)$ is the time scale for a disturbance at $y = \Delta_y$ to reach $y = 0$. The filtered flow field is fully resolved by the LES grid (see Bose & Moin, 2014). Hence,

$$u \approx u_w + \frac{u_{\text{LES}} - u_w}{h_{wm}} y, \;\; p \approx p_w + \frac{p_{\text{LES}} - p_w}{h_{wm}} y, \;\; 0 < y < h_{wm}. \tag{14}$$

The integration in Eq. 12 then becomes trivial. It is worth noting that such a simplification cannot be exploited in the integral model. This is because in Yang *et al.* (2015), the LES filter acts only in the x and z directions and the near wall sub-grid velocity comprises a linear inner layer and a log meso-layer along with an additional linear term. In this work, Eq. (12) is used along with the Robin-type closure, however, such a correction is in principle applicable to any LES wall model that is based on the law of wall. This falls out of the scope of this paper and is left for future investigation.

LES SETUP

We use the open-source incompressible flow solver LESGO (publically available on github). Details of this pseudo-spectral code can be found in Bou-Zeid *et al.* (2005) and Anderson & Meneveau (2011). We solve for flow in an open half-channel. A constant pressure gradient is imposed in the streamwise direction. The friction velocity u_τ is known from $u_\tau = \sqrt{-1/\rho \partial \langle p \rangle / \partial x}$, where $\rho = Const$ is the fluid density and p is the dynamic pressure. A symmetric boundary condition is used on the top boundary. Spanwise and streamwise periodicities are imposed. The computational

domain is of size $2\pi\delta \times \delta \times 2\pi\delta$ in the x, y, z directions, respectively, where $\delta = 1$ is the half-channel height. Four LES wall models are examined: the algebraic equilibrium wall model (Eq. 2), the integral wall model (Yang *et al.*, 2015), the equilibrium slip wall model (Eq. (10)) and the non-equilibrium slip wall model (Eq. (11)). Both the algebraic equilibrium model and the integral wall model are readily available in the code. To investigate the effects of grid resolution, two mesh sizes, 64^3 and 128^3, are considered. Uniform grid spacing is used in all directions. Three dynamic sub-grid scale (SGS) models including the dynamic Smagorinsky model (Germano *et al.*, 1991), the dynamic Lagrangian Smagorinsky model (Meneveau *et al.*, 1996) and the scale-dependent dynamic Lagrangian Smagorinsky model (Bou-Zeid *et al.*, 2005), are considered. All the SGS models are already implemented in the code. The half channel is at a friction Reynolds number $Re_\tau = 4200$, where $Re_\tau = \delta u_\tau/\nu$ and ν is the kinematic viscosity. A full-channel DNS at this Reynolds number is reported in Lozano-Durán & Jiménez (2014). The viscous length scale to be used in the algebraic equilibrium wall model is $y_o = \nu/u_\tau \exp(-\kappa B)$, where $B = 5$ according to the law of wall.

EFFECTS OF WALL MODELS

Figure 1 (a) shows the mean velocity profiles as functions of the wall-normal distance. All the WMLES in figure 1 have used a grid of size 128^3 and the sub-grid scale (SGS) stresses are all modeled using the scale-dependent dynamic Lagrangian Smagorinsky model. A slightly positive log-layer mismatch is found for the two slip wall models. Overall, the law of wall is captured irrespect of the wall model used.

Figure 1 (b) shows the variance of the streamwise velocity fluctuation as functions of the wall-normal distance. The DNS results are included for comparison. LES solves the filtered Navier-Stokes (NS) equation. For a fair comparison, we also filter the DNS using a top hat filter of size $\Delta x^+ \times \Delta y^+ \times \Delta z^+ \approx 200 \times 32.8 \times 200$, which commensurate with the resolution of the WMLES. At high Reynolds numbers, the streamwise variance follows a logarithmic scaling in the log region (Hultmark *et al.*, 2012). However, at this Reynolds number ($Re_\tau = 4200$), one can barely find a log region in $\left\langle u'^2 \right\rangle$. In the near-wall region, WMLES are more comparable to the DNS than the filtered DNS. In the bulk region, the filtered DNS, the DNS and the WMLES are not very different. The two Robin-type wall models lead to $\left\langle u'^2 \right\rangle$ profiles that are closer the filtered DNS results, while the integral wall model and the equilibrium wall model result in profiles that agree better with the DNS results. At this Reynolds number, for the particular grid and SGS model, it seems that neither the mean velocity nor the streamwise variance depends critically on wall models.

EFFECTS OF SGS MODELS

The mean velocities follow the log law closely when different SGS models are used (not shown for brevity). Figure 2 shows the streamwise variance as functions of the wall normal distance. All WMLES in figure 2 have used a grid of size 128^3. For brevity, only the integral wall model results and the equilibrium slip wall model results are shown. When the equilibrium slip wall model is used, SGS models do not seem to make a big difference in the bulk region and the WMLES results agree reasonably well with the filtered DNS. On the other hand, when the integral model is used, Lagrangian models lead results that agree with the DNS and the non-Lagrangian model leads to a profile that follows the filtered DNS results. In the near wall region, different SGS models lead to distinctly different turbulence intensities.

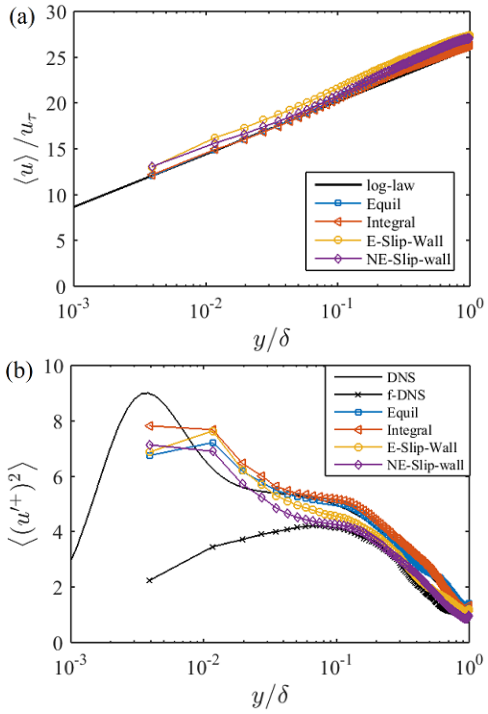

Figure 1. (a) Mean velocity profiles as functions the wall-normal distance. The log-law corresponds to $U/u_\tau = 1/\kappa \log(yu_\tau/\nu) + B$, with $\kappa = 0.4$, $B = 5$. "Equil" is for the algebraic equilibrium wall model, "Integral" is for the integral wall model, "E-Slip-Wall" is for the equilibrium slip wall model, "NE-Slip-Wall" is for the non-equilibrium slip wall model and "f-DNS" is for the filtered DNS. (b) Same as (a) but for the streamwise variance.

EFFECTS OF GRID RESOLUTION

The law of wall is captured at both grids, 64^3 and 128^3. Results of the mean flow are therefore not shown for brevity. Figure 3 (a–c) show the variance of the streamwise fluctuation as functions of the wall-normal distance for the algebraic equilibrium wall model, the integral wall model and the equilibrium slip wall model, respectively. All WMLES cases in figure 3 have used the scale-dependent Lagrangian Smagorinsky model for SGS stress modeling. When a large grid is used (in this case, a grid size of 128^3), the results are fairly insensitive to the choice of wall model. However, wall models start to make a difference when a coarse grid is employed (in this case, 64^3).

The expected convergence of the LES streamwise variance to DNS is from $y = \delta$ to the wall. This is because first that for $\left\langle u'^2 \right\rangle$ at a wall-normal height y, only eddies whose heights are greater than $O(y)$ are statistically significant (see Townsend (1976); Woodcock & Marusic (2015); Yang *et al.* (2016*a*,*b*) for detailed discussion) and second that as the grid gets refined, large-scale flow structures get resolved first and then the small-scale structures. This expected trend is observed when the integral wall model or the equilibrium slip wall model is used. However, for the algebraic equilibrium wall model, when a coarse grid is used, the streamwise variance deviates from the DNS profile even in the bulk region, suggesting a poorly resolved bulk region. These observations suggest that the integral wall model and the equilibrium slip wall model lead to more realistic flow structures than the algebraic equilibrium wall model when a coarse grid is employed.

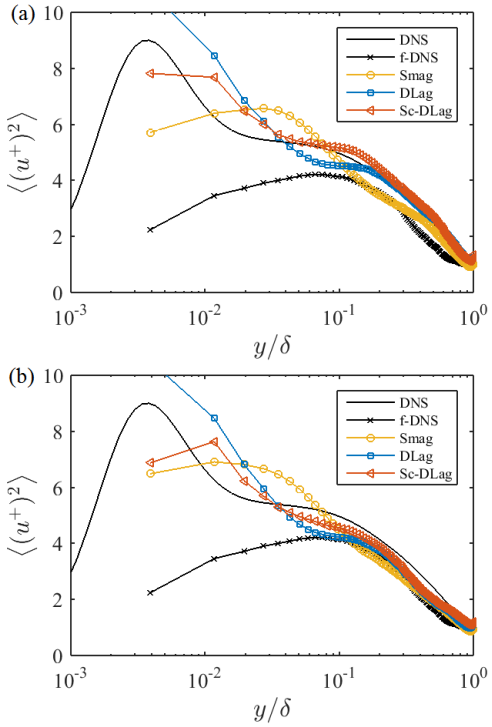

Figure 2. (a) The streamwise variance as functions of the wall normal distance from WMLES that use the integral wall model for near-wall modeling. The dynamic Smagorinsky model (Smag), the dynamic Lagrangian Smagorinsky model (DLag) and the scale-dependent dynamic Lagrangian Smagorinsky model (Sc-DLag) are used for SGS stress modeling. "f-DNS" is for the filtered DNS. (b) Same as (a) but for the equilibrium slip wall model.

THE INSTANTANEOUS WALL SHEAR STRESS

Figure 4 shows the instantaneous wall shear stress contours from the filtered DNS and the WMLES with various wall models. All WMLES in this section use a grid of size 128^3 and SGS stresses are modeled using the scale-dependent Lagrangian Smagorinsky model. Although streaky structures can be seen independent of the wall closure used, the spatial distribution of the fluctuating wall stress depends very much on the choice of LES wall model. Visually, compared to the other two wall models considered here, the integral wall model leads to wall shear stress that resembles the filtered DNS stress the most.

Both the algebraic equilibrium wall model as well as the equilibrium slip wall model relate the wall shear stress to the local LES velocity. For equilibrium wall model $\tau_{w,x} \sim u_\tau^2 \sim u_{\text{LES}}^2$ and for the slip wall model $\tau_{w,x} \sim \nu_T \partial u/\partial y \sim \nu_T u_{\text{LES}} \sim u_{\text{LES}}$, where u_{LES} is the LES velocity at $y = h_{wm}$. Wall shear stresses computed according to the integral wall model and the non-equilibrium slip wall model, on the other hand, do not depend only on u_{LES}, but also on the LES solutions in the neighboring computational cells. Figure 5 are scatter plots of the instantaneous wall shear stress as functions of the square of the velocity at $y = h_{wm}$. Overall, the instantaneous wall shear stress is positively correlated with the velocity at $y = h_{wm}$. A good amount of scattering is found in the filtered DNS data and the scattering becomes more significant at large $u(y = h_{wm})$ values. The scattering in WMLES cases are quite moderate with most $\left([u(y = h_{wm})/(\langle u(y = h_{wm})\rangle)]^2, \tau_w/u_\tau^2\right)$ pairs center around $(1,1)$. The least square fit of the data in figure 5 (b, c) reduces to the their equilibrium counterparts, $\tau_w \sim u_{\text{LES}}^2$ and $\tau_w \sim u_{\text{LES}}$, respectively.

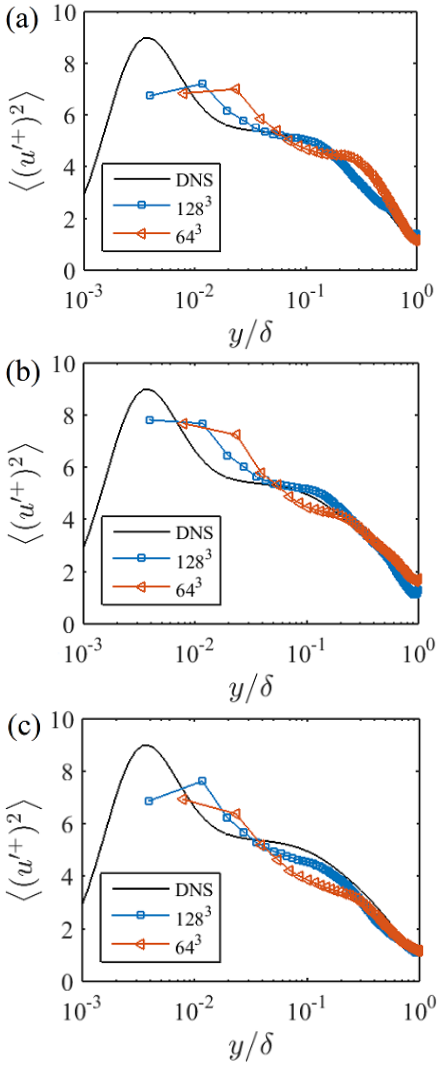

Figure 3. Variance of the streamwise velocity fluctuations as functions of the wall-normal distance at two grids 64^3 and 128^3 for WMLES that use (a) the algebraic equilibrium wall model, (b) the integral wall model, (c) the equilibrium slip wall model. DNS data are shown for comparison.

Figure 6 shows the p.d.f. of the wall stress. Although the algebraic equilibrium wall model and the equilibrium slip wall model are both based on equilibrium considerations, the resulting wall shear stress p.d.f.'s are noticeably different. Because fluctuations in the wall shear stress are correlated with local flow acceleration and local pressure gradient, even for the equilibrium channel flow considered here, accounting for non-equilibrium effects helps in capturing the p.d.f. of the wall shear stress. The wall shear stress p.d.f. resulted from the integral wall model is in close agreement with that of the filtered DNS. This result is quite encouraging, yet, it is not entirely unexpected considering the success of the integral wall model in the *a priori* test reported in Graham *et al.* (2016). Compared with the wall shear stress of the filtered DNS, the p.d.f. resulted from the equilibrium wall model is slightly less peaked and the p.d.f. resulted from the equilibrium slip wall model is slightly more peaked. This is not unexpected because the p.d.f. of u_{LES}^2 (according to the equilibrium wall model $\tau_w \sim u_{\text{LES}}^2$) is certainly less peaked than that of u_{LES} (according to the equilibrium slip wall model $\tau_w \sim u_{\text{LES}}$). Last, by including the non-equilibrium effects, the wall stress p.d.f. becomes less peaked. The wall stress p.d.f. from the DNS is in-

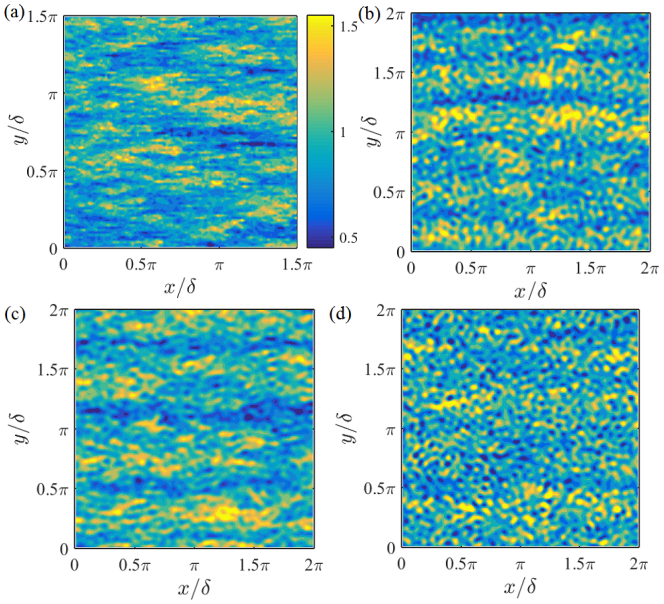

Figure 4. Contour plots of the normalized instantaneous streamwise wall shear stress, $\tau_{w,x}/u_\tau^2$ from (a) the filtered DNS (b) WMLES with the equilibrium wall model (c) WMLES with the integral wall model and (d) WMLES with the non-equilibrium slip-wall model.

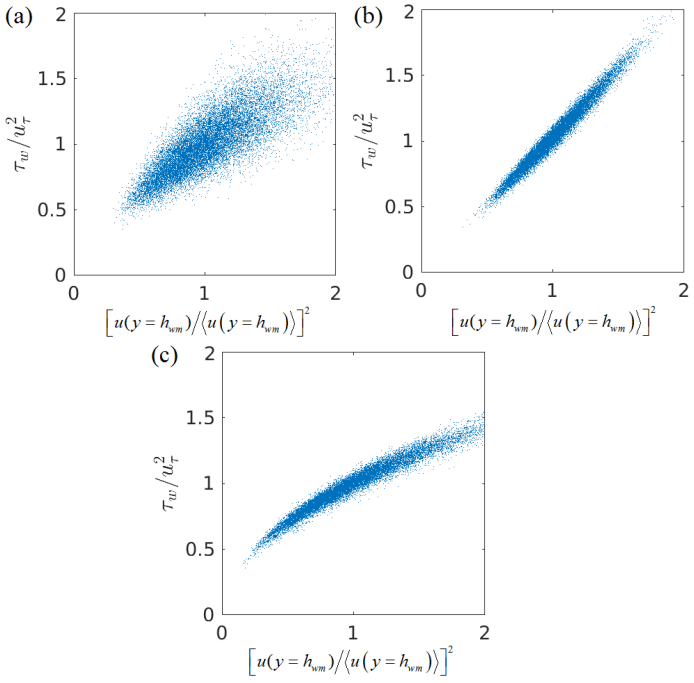

Figure 5. Scatter plots of the instantaneous wall shear stress as functions of the square of the velocity at $y = h_{wm}$. (a) the filtered DNS. (b) WMLES with the integral wall model, (c) WMLES with the non-equilibrium slip wall model.

cluded in figure 6 for comparison; although it is not expected that with a typical LES grid, this p.d.f. can be captured.

Conclusions

A physics-based interpretation is provided for the slip-wall closures by Bose & Moin (2014). The slip wall model, which was

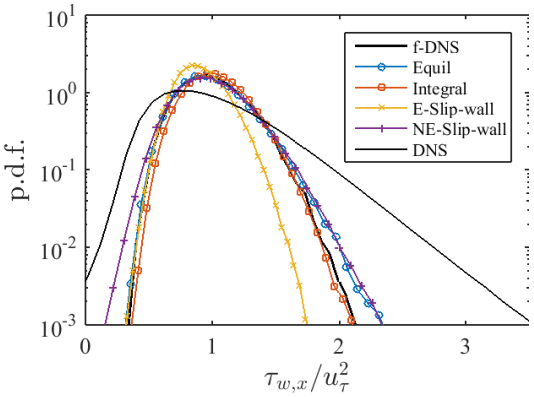

Figure 6. The streamwise wall stress p.d.f. from WMLES, DNS and filtered DNS. f-DNS is filtered DNS. The other legends are the same as those in figure 1.

previously associated with the use of the differential filter in LES, is found to be compatible with arbitrary LES filter. Numerical experiments in this work suggest that the physics-based interpretation here is reasonable and the Robin-type wall closure, with a properly picked length scale l_p, can be used as an alternative to the conventional wall models that supply the wall shear stress directly. The model performance is examined in turbulent channel flow and compared against the algebraic equilibrium wall model and the algebraic integral wall model. The flow quantities of interest include the mean velocity, the streamwise variance and the instantaneous wall shear stress. When a sufficiently large grid is used, both the mean velocity and the variance of the streamwise velocity fluctuation do not depend critically on the LES wall model, at least for the wall models tested in this work. However, when a coarse-grid is used, the integral wall model and the slip wall model appear to give a more realistic prediction of the streamwise variance than the algebraic equilibrium wall model. The p.d.f. of the wall shear stress depends sensitively on the wall model. The tests here show that for channel flow at the particular Reynolds number $Re_\tau = 4200$, the integral wall model captures quite well the p.d.f. of the filtered wall stress. Whether this holds for a different flow configuration, at a different Reynolds number and at a different grid resolution is not entirely clear and further investigations will be needed. As for the slip wall models, explicitly accounting for non-equilibrium effects is useful even for equilibrium flows like channel flow because the extreme wall shear stresses are likely to be correlated with local flow acceleration and local pressure gradient.

To conclude the discussion, we briefly discuss how the effects of sub-grid roughness can be accounted for in a Robin-type LES wall closure. In the pioneering work by Bose & Moin (2014), it is pre-assumed that the wall is smooth. As the effects of roughness are commonly parameterized using a darg force $-C_d U^2$ in the momentum equation, accounting for sub-grid roughness is highly non-trivial without referring to the NS equation. In this work, because we have related the Robin-type wall condition to the NS equation, the effects of roughness can be accounted for by adding a drag force term to Eq. (5) or simply by using an effective roughness length y_o in Eq. (6).

Acknowledgements

The work was funded by the US AFOSR (Grant No. 1194592-1-TAAHO). XY is grateful to C. Meneveau, A. Lozano-Duran and H. J. Bae for their helpful suggestions and fruitful discussions.

REFERENCES

Anderson, W & Meneveau, C 2011 Dynamic roughness model for large-eddy simulation of turbulent flow over multiscale, fractal-like rough surfaces. *J. Fluid Mech.* **679**, 288–314.

Balaras, E & Benocci, C 1994 Subgrid-scale models in finite-difference simulations of complex wall bounded flows. *AGARD CP* **551** (2.1).

Bazilevs, Y & Hughes, Thomas J R 2007 Weak imposition of dirichlet boundary conditions in fluid mechanics. *Computers & Fluids* **36** (1), 12–26.

Bose, S T & Moin, P 2014 A dynamic slip boundary condition for wall-modeled large-eddy simulation. *Phys. Fluids* **26** (1), 015104.

Bou-Zeid, Elie, Meneveau, C & Parlange, Marc 2005 A scale-dependent Lagrangian dynamic model for large eddy simulation of complex turbulent flows. *Phys. Fluids* **17** (2), 025105.

Bou-Zeid, E, Meneveau, C & Parlange, M B 2004 Large-eddy simulation of neutral atmospheric boundary layer flow over heterogeneous surfaces: Blending height and effective surface roughness. *Water Resources Research* **40** (2).

Chapman, D R 1979 Computational aerodynamics development and outlook. *AIAA J.* **17** (12), 1293–1313.

Choi, H & Moin, P 2012 Grid-point requirements for large eddy simulation: Chapman's estimates revisited. *Phys. Fluids* **24** (1), 011702.

Chung, D & Pullin, D I 2009 Large-eddy simulation and wall modelling of turbulent channel flow. *J. Fluid Mech.* **631**, 281–309.

Germano, M, Piomelli, U, Moin, P & Cabot, W H 1991 A dynamic subgrid-scale eddy viscosity model. *Phys. Fluids* **3** (7), 1760–1765.

Graham, J, Kanov, K, Yang, X I A, Lee, M, Malaya, N, Lalescu, CC, Burns, R, Eyink, G, Szalay, A, Moser, R D *et al.* 2016 A web services accessible database of turbulent channel flow and its use for testing a new integral wall model for LES. *J. Turbul* **17** (2), 181–215.

Hultmark, M, Vallikivi, M, Bailey, S C C & Smits, A J 2012 Turbulent pipe flow at extreme reynolds numbers. *Phys. Rev. Lett.* **108** (9), 094501.

Kawai, Soshi & Larsson, Johan 2012 Wall-modeling in large eddy simulation: Length scales, grid resolution, and accuracy. *Phys. Fluids* **24** (1), 015105.

Lozano-Durán, A & Jiménez, J 2014 Effect of the computational domain on direct simulations of turbulent channels up to Re_τ= 4200. *Phys. Fluids* **26** (1), 011702.

Meneveau, C, Lund, T S & Cabot, W 1996 A Lagrangian dynamic subgrid-scale model of turbulence. *J. Fluid Mech.* **319**, 353–385.

Nicoud, F, Baggett, J S, Moin, P & Cabot, W 2001 Large eddy simulation wall-modeling based on suboptimal control theory and linear stochastic estimation. *Phys. Fluids* **13** (10), 2968–2984.

Park, G I & Moin, P 2014 An improved dynamic non-equilibrium wall-model for large eddy simulation. *Phys. Fluids* **26** (1), 015108.

Piomelli, U & Balaras, E 2002 Wall-layer models for large-eddy simulations. *Ann. Rev. Fluid Mech.* **34** (1), 349–374.

Porté-Agel, F, Meneveau, C & Parlange, M B 2000 A scale-dependent dynamic model for large-eddy simulation: application to a neutral atmospheric boundary layer. *J. Fluid Mech.* **415**, 261–284.

Schumann, U 1975 Subgrid scale model for finite difference simulations of turbulent flows in plane channels and annuli. *J Comput Phys* **18** (4), 376–404.

Templeton, J A, Wang, M & Moin, P 2006 An efficient wall model for large-eddy simulation based on optimal control theory. *Phys. Fluids* **18** (2), 025101.

Townsend, A A 1976 The structure of turbulent shear flows. *Cambridge University Press, Cambridge, UK* .

Woodcock, J D & Marusic, I 2015 The statistical behaviour of attached eddies. *Phys. Fluids* **27** (1), 015104.

Yang, X I A, Marusic, I & Meneveau, C 2016*a* Hierarchical random additive process and logarithmic scaling of generalized high order, two-point correlations in turbulent boundary layer flow. *Phys. Rev. Fluids* **1** (2), 024402.

Yang, X I A, Meneveau, C, Marusic, I & Biferale, L 2016*b* Extended self-similarity in moment-generating-functions in wall-bounded turbulence at high Reynolds number. *Phys. Rev. Fluids* **1** (4), 044405.

Yang, X I A, Sadique, J, Mittal, R & Meneveau, C 2015 Integral wall model for large eddy simulations of wall-bounded turbulent flows. *Phys. Fluids* **27** (2), 025112.